POLYTECHNIQUE MONTRÉAL

WORLD-CLASS ENGINEERING

IZA Program – ZCO-72
Surface Profile Effects on AHSS processing

Presented by : Paul Mosser, Kyle Daun and Myriam Brochu

Prepared by: Paul Mosser, Marina Pushkareva, Quentin Somveille, Kyle Daun and Myriam Brochu

In collaboration with:

UNIVERSITY OF WATERLOO

McMaster University

GAP Meeting – October 2017

Contents

1.1 Goal of ZCO-72 project

Industrial Challenge:

High rejection rates of Advanced High-Strength Steel (AHSS) strip processed in Continuous Galvanizing Lines (CGLs).

Hypothesis based on literature:

I. AHSS are more sensitive than conventional steels to any deviation in time and temperature, through emissivity-induced pyrometry errors, during annealing and tempering.

II. Variability in the surface condition (oxidation, roughness, thickness, defects, microstructure) of AHSS affects emissivity and thus process temperature and consequently mechanical properties and zinc adherence.

Ultimate goal:

Study the influence of **steel strips surface characteristics** on both the mechanical properties and the coating quality of hot dip galvanized AHSS, **by focusing on emissivity variations.**

1.2 Basics of pyrometry

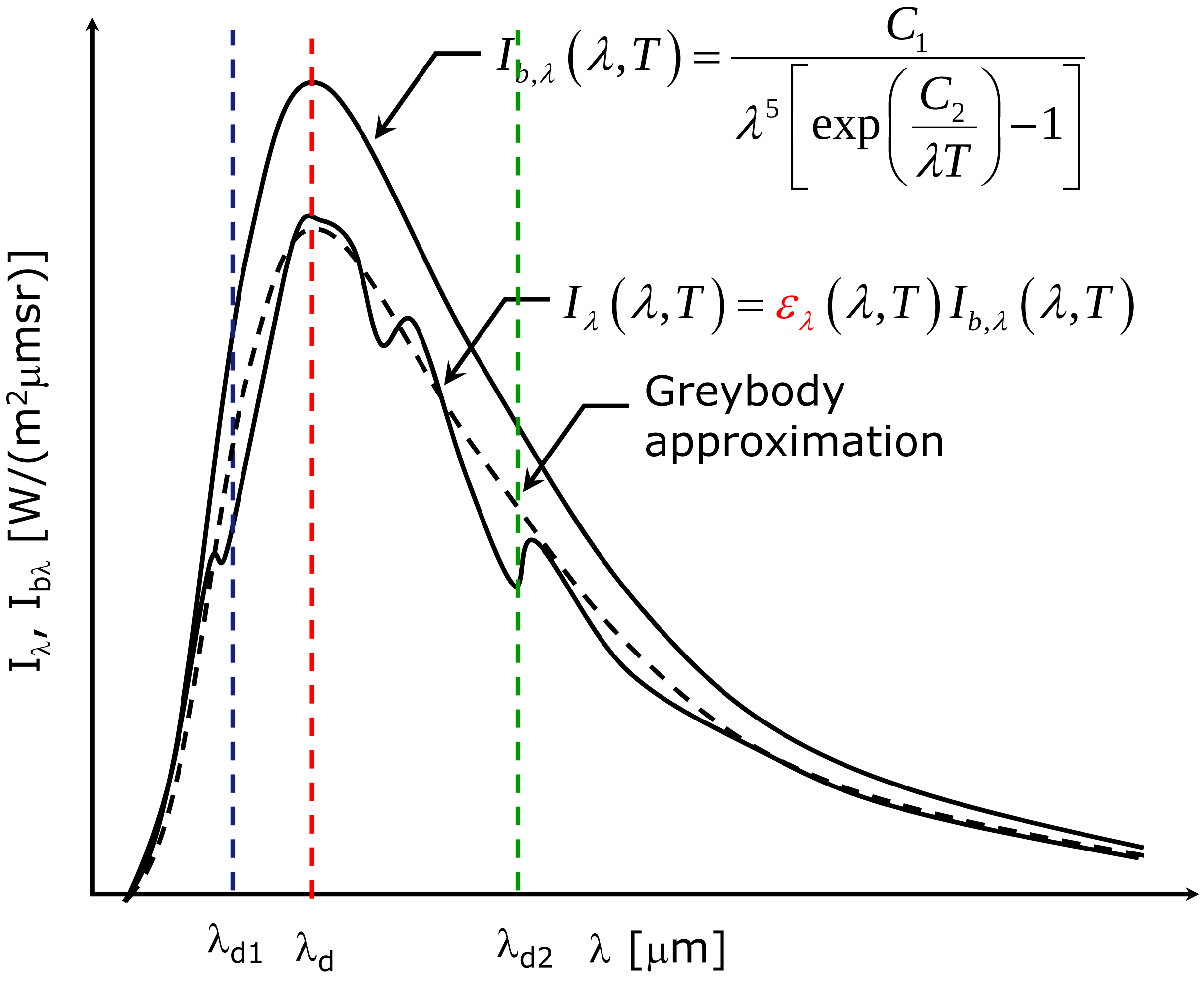

Fig. 1: Influence of emissivity on spectral radiative intensity.

Monochromatic pyrometry

$$I_\lambda(\lambda_d,T) \approx \frac{\varepsilon_\lambda C_1}{\lambda_d^5\left[\exp\left(\frac{C_2}{\lambda_d T}\right)-1\right]}$$

$$T = \frac{C_2}{\lambda_d \ln\left[\left(\frac{\varepsilon_\lambda C_1}{\lambda^5 I_\lambda}\right)+1\right]}$$

Two-color (ratio) pyrometry

$$\frac{I_{\lambda1}(\lambda,T)}{I_{\lambda2}(\lambda,T)} \approx \frac{\varepsilon_{\lambda1}}{\varepsilon_{\lambda2}}\left(\frac{\lambda_2}{\lambda_1}\right)^5 \exp\left[\frac{C_2}{T}\left(\frac{1}{\lambda_2}-\frac{1}{\lambda_1}\right)\right]$$

$$T = \frac{C_2\left(\frac{1}{\lambda_2}-\frac{1}{\lambda_1}\right)}{\ln\left[\frac{\varepsilon_{\lambda2}}{\varepsilon_{\lambda1}}\left(\frac{\lambda_1}{\lambda_2}\right)^5 \frac{I_{\lambda1}(\lambda,T)}{I_{\lambda2}(\lambda,T)}\right]}$$

= 1 for greybody

T depends on ε_λ

1.3 Heat treatment cycles

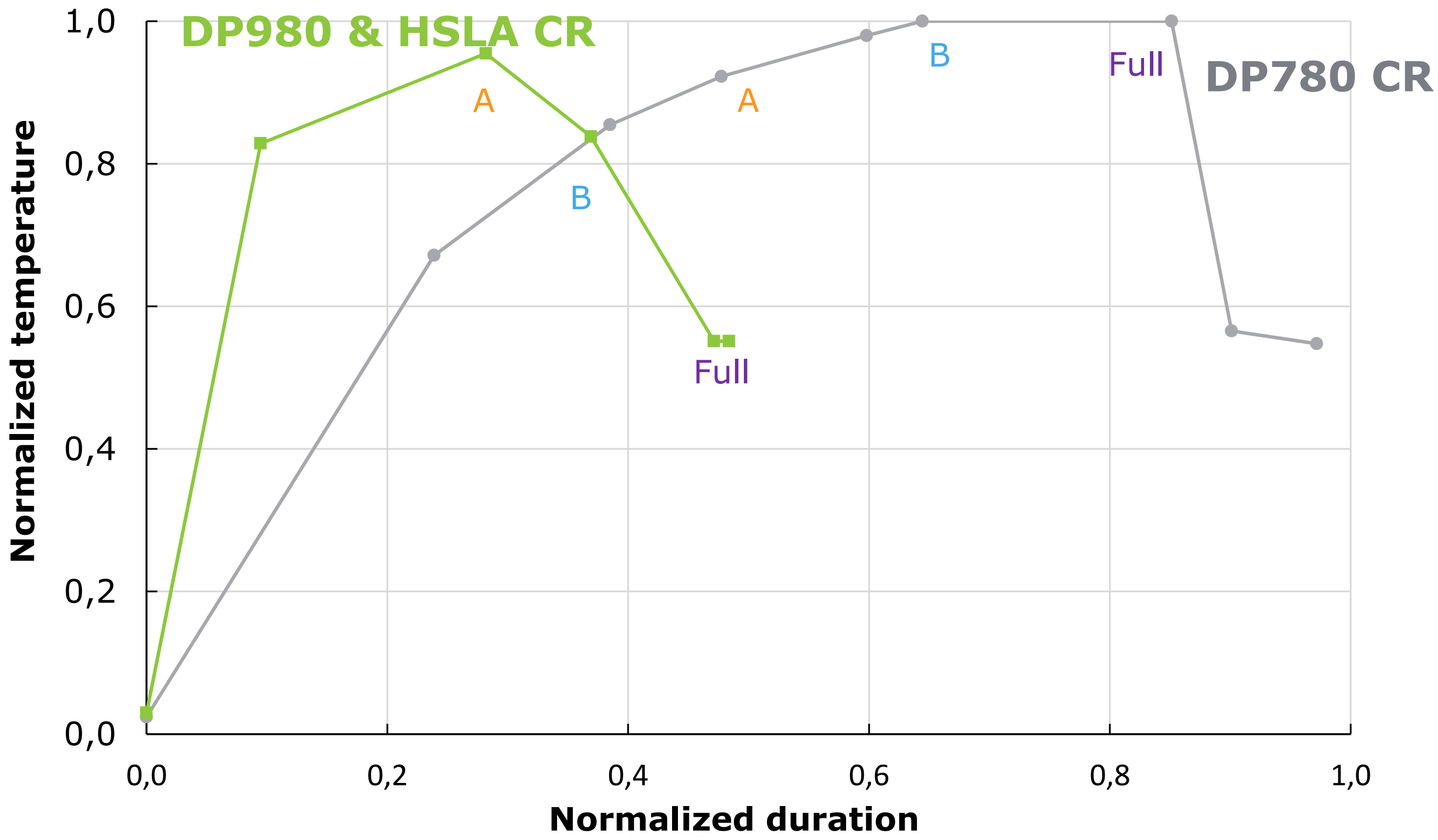

Fig. 2 : Phase I Heat Treatment Cycles with interruptions A and B.

Table. 1 : Summary of the studied materials and dew points.

Materials	Dew Point
HSLA CR	
DP780 CR	-30°C 0°C
DP980 CR	

1.4 Follow-up: non-uniform temperatures

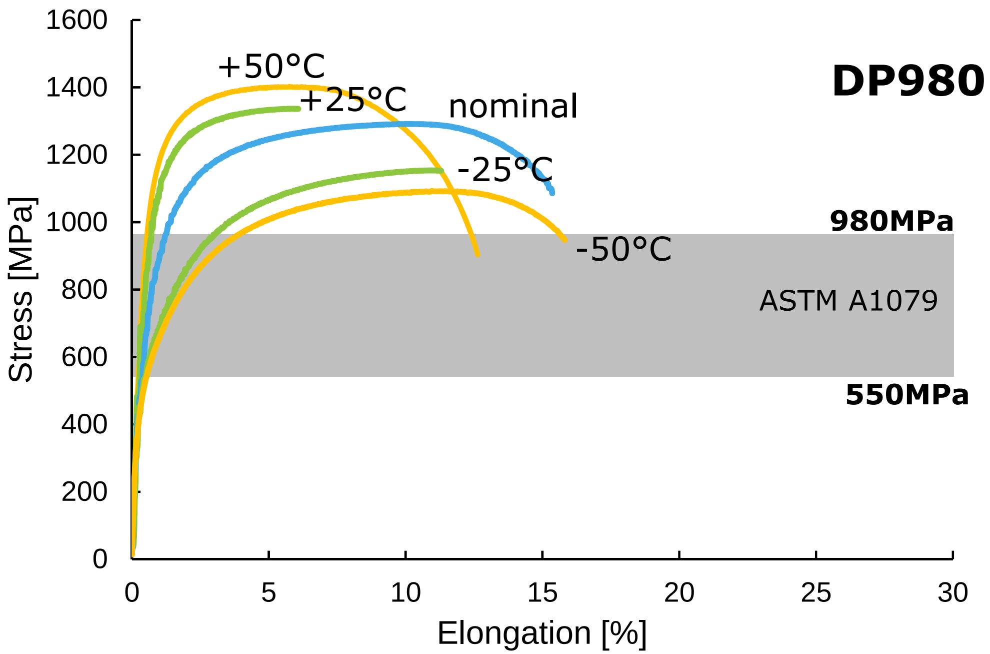

Fig. 3: Stress – Strain curves for DP980 all condition.

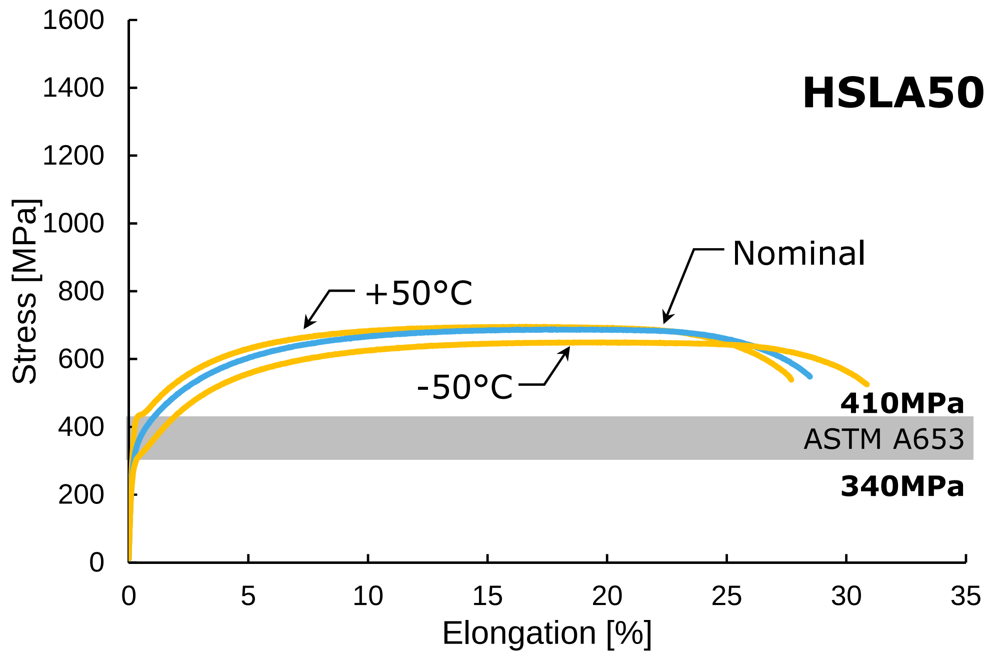

Fig. 4: Stress – Strain curves for HSLA all condition.

- Temperature is nearly uniform over a 90mm x 90mm area in the lower portion of panel[1)].
- New observations have been performed with samples extracted from this area.

1) E.M. Bellhouse, A.I.M. Mertens, J.R. McDermid, « Development of the surface structure of TRIP steels prior to hot-dip galvanizing », Mat. Sc. and Eng. A, 463, 2007

1.4 Follow-up non-uniform temperatures – DP980

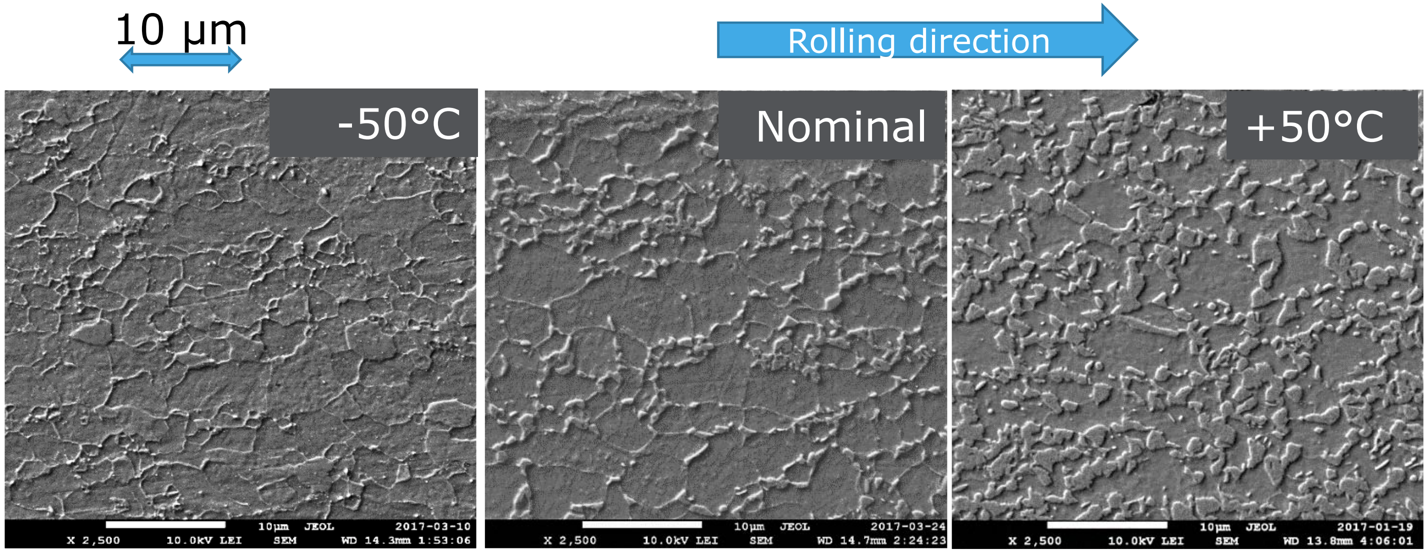

Fig. 5: SEM observation of DP980.

Microstructure:
Ferrite – Martensite

Table 2: Ferrite surface ratio and grain size of ferrite for DP980.

Heat Cycle		-50°C	-25°C	Nominal	+25°C	+50°C
Ferrite surface ratio [%]		65 (92)	59 (79)	42 (81)	26 (80)	<5 (52)
Mean intercept length [µm]	Rolling direction	3.0 (3.5)	3.5 (3.1)	2.3 (3.2)	2.2 (3.4)	NA (2.6)
	Transverse direction	2.1 (2.8)	2.4 (2.5)	1.8 (2.6)	1.7 (2.3)	NA (2.2)

() = previous results on coupons located near the edges

- The proportion of ferrite decreases with increasing annealing temperature.
- Ferrite grain size is comparable for all specimens except for +50°C condition, where it was not possible to measure.

Revised microstructure evolution is more consistent with mechanical properties.

1.4 Follow-up non-uniform temperatures – HSLA

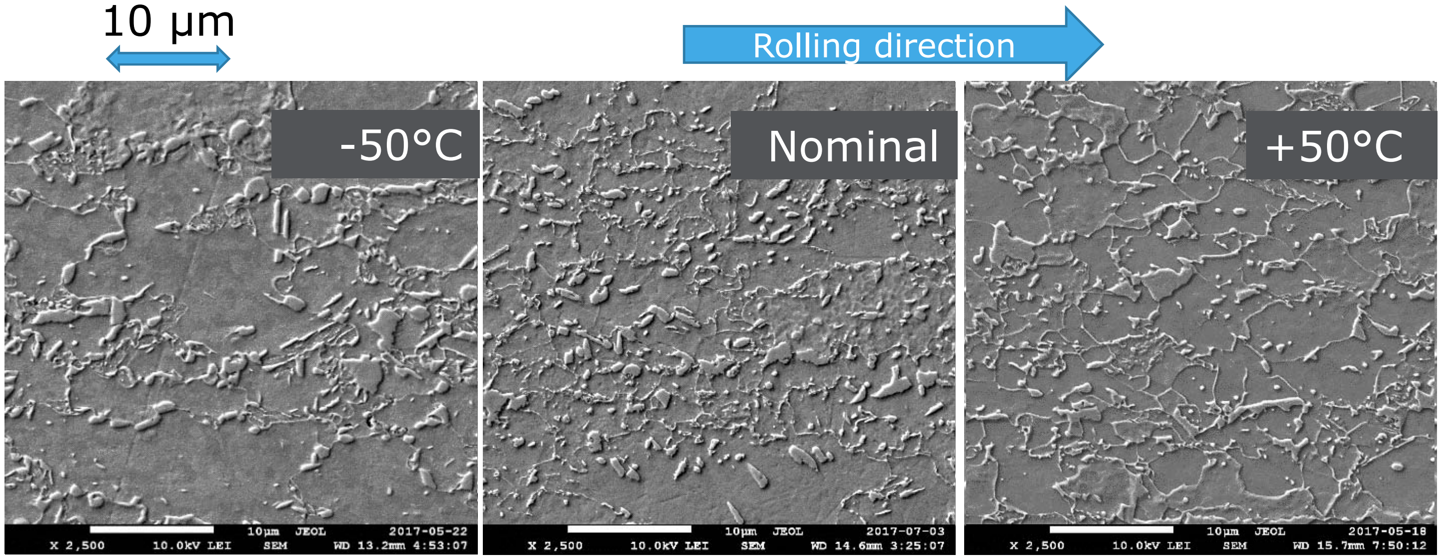

Fig. 6: SEM observation of HSLA.

Microstructure:
Ferrite – Martensite

Table 3: Ferrite surface ratio and grain size of ferrite for HSLA.

Heat Cycle		-50°C	Nominal	+50°C
Ferrite surface ratio [%]		81 (none)	77 (none)	75 (none)
Mean intercept length [µm]	Rolling direction	8.6 (10.2)	6.5 (8.1)	5.1 (8.3)
	Transverse direction	5.6 (5.3)	4.4 (5.2)	4.1 (5.6)

() = previous results on coupons located near the edges

- Ferrite ratio decreases with increasing annealing temperature.

- Ferrite grain size is comparable for nominal and +50°C condition and larger for -50°C condition.
- Grain anisotropy decreases with increasing temperature.

1.4 Follow-up: size effects

Hypothesis: subsize specimen may cause over-estimated elongation-at-failure.

DP980 – Nominal heat cycle

Table 4: Elongation comparison with extensometer and DIC method for subsize and standard DP980 tensile specimen.

Specimen size	Extenso - E%	DIC - E%
Subsize – 25mm	14%	15%
Standard – 50mm	-	14%

HSLA – Nominal heat cycle

Table 5: Elongation comparison with extensometer and DIC method for subsize and standard HSLA tensile specimen.

Specimen size	Extenso - E%	DIC - E%
Subsize - 25mm	28%	29%
Standard – 50mm	-	28%

- Previous conclusion comes from virtual extensometer of different initial length placed on standard size specimen.
- **Following experimental results no significant size effect was observed.**

Future work: Confirm result for other heat treatment cycles

2.1 Impact of dew point on emissivity

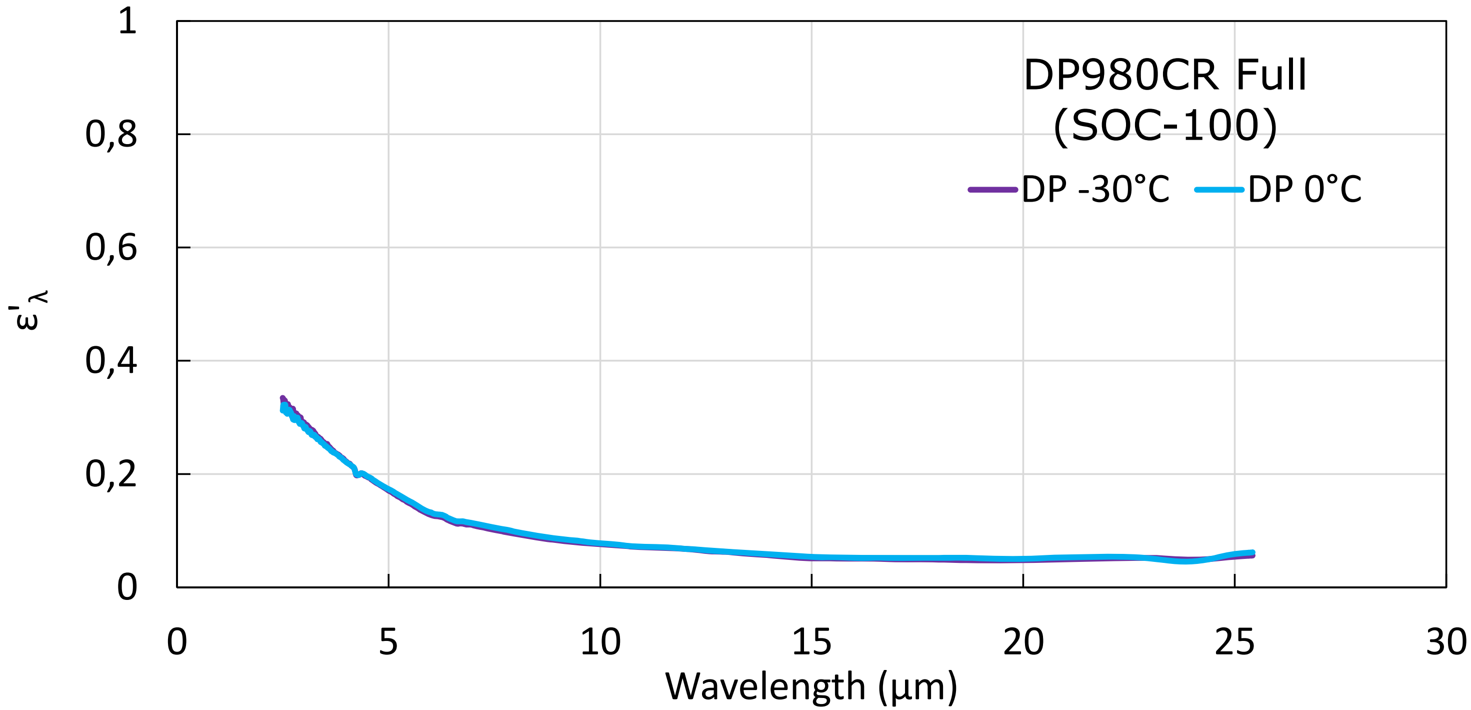

Fig. 7: Emissivity at long wavelengths of DP980CR "Full" for dew points of -30°C and 0°C.

No influence of the dew point on DP980 long wavelengths emissivity (λ>2.5µm) (GAP Meeting Oct. 2016).

2.1 Impact of dew point on emissivity

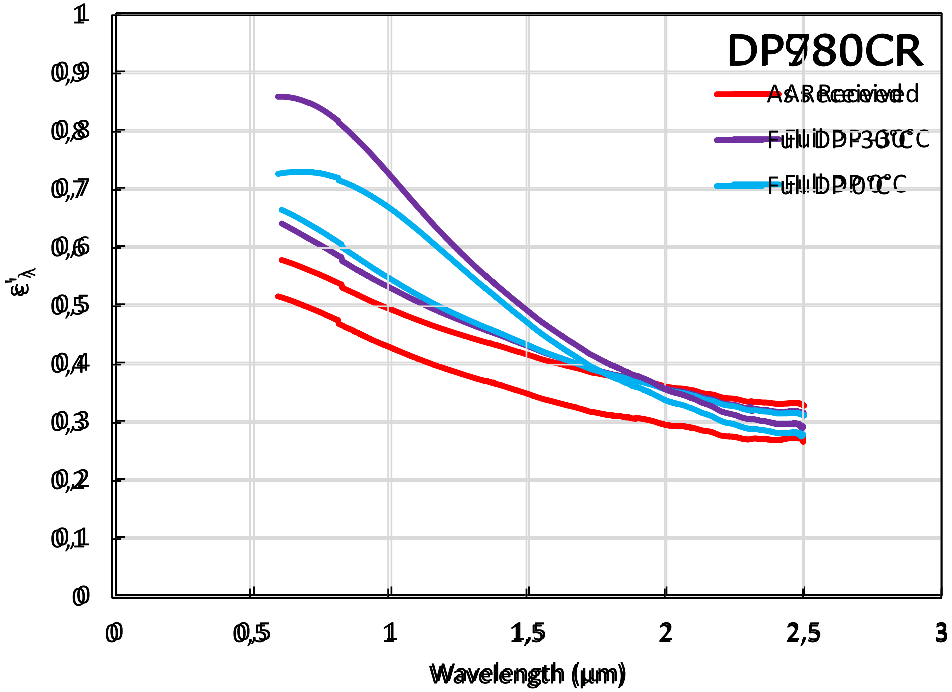

Fig. 10: Emissivity at short wavelengths of DP780CR heated with dew points of -30°C and 0°C.

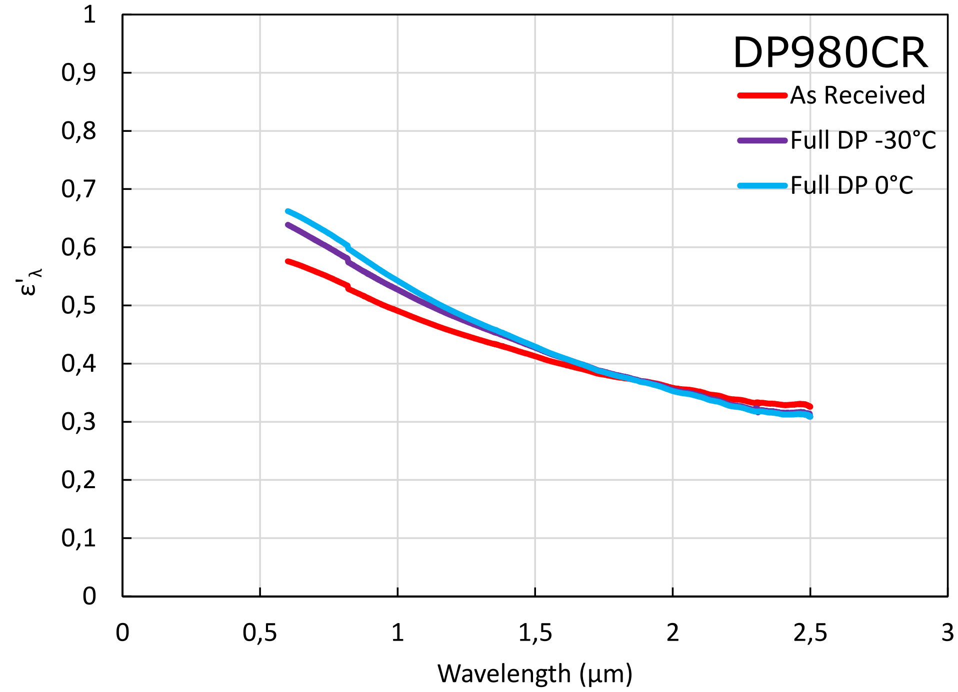

Fig. 8: Emissivity at short wavelengths of DP980CR heated with dew points of -30°C and 0°C.

Changing the dew point from -30°C to 0°C slightly increases the evolution of emissivity during the heat treatment for DP980CR for wavelengths shorter than 1µm.

Changing the dew point from -30°C to 0°C reduces the evolution of emissivity during the heat treatment for DP780CR.

2.1 Impact of dew point on emissivity

Full DP -30°C

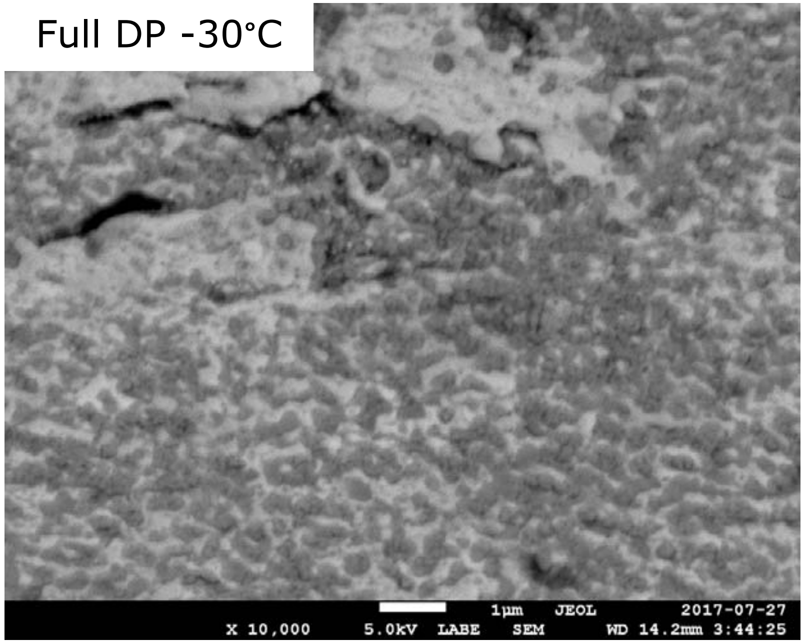

Fig. 12: SEM image of DP780 "Full" with a dew point of -30°C.

DP780CR

Full DP 0°C

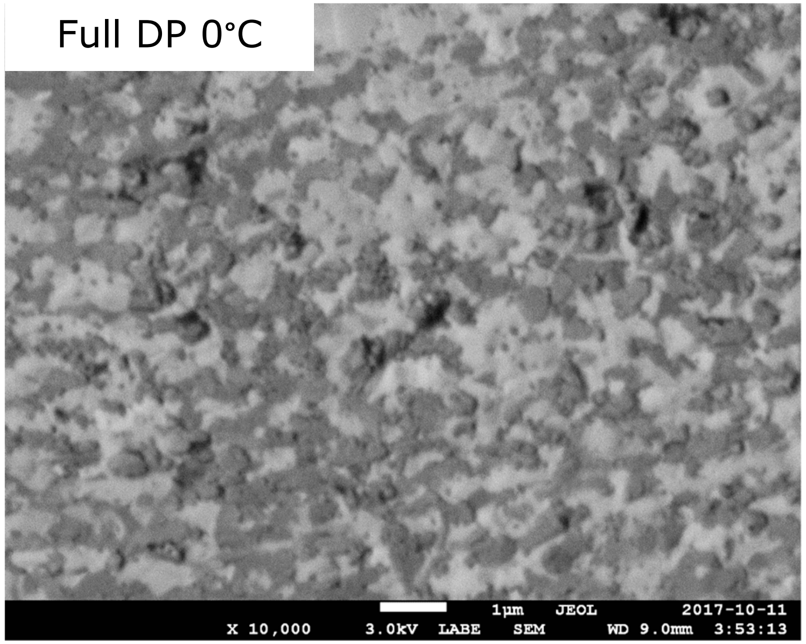

Fig. 13: SEM image of DP780 "Full" with a dew point of 0°C..

When changing the dew point from -30°C to 0°C:
- Bigger oxide islands
- Wider spacing between islands
- Transition from external to internal oxidation [2)]

2) I-R. Sohn, J-S. Kim, S. Sridhar "Effect of Dew points and Gas Flow Rate on the Surface Oxidation of Advanced High Strength Steels", ISIJ Int., Vol. 55(2015), No. 9.

2.2 Oxide morphology

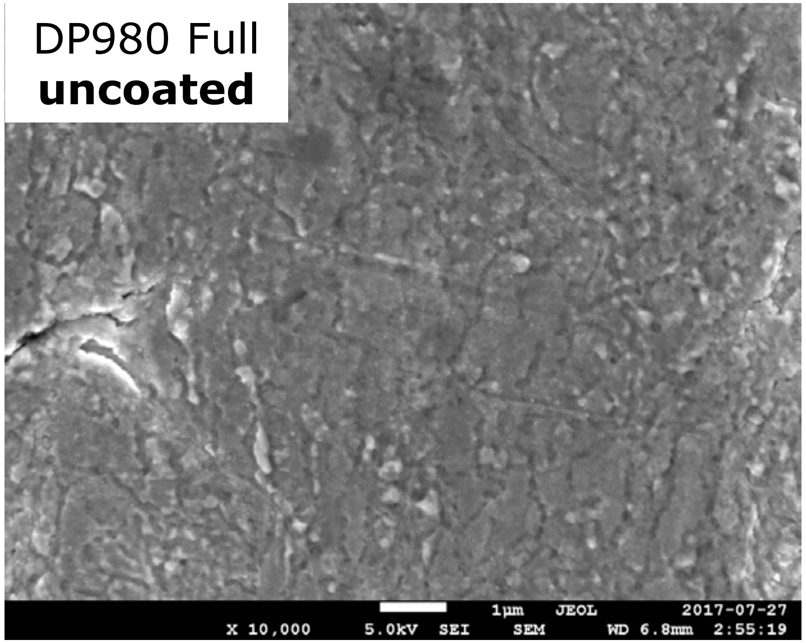

Fig. 14: SEM image of DP980 Full DP-30°C, uncoated.

Improving image quality, work performed in collaboration with McMaster

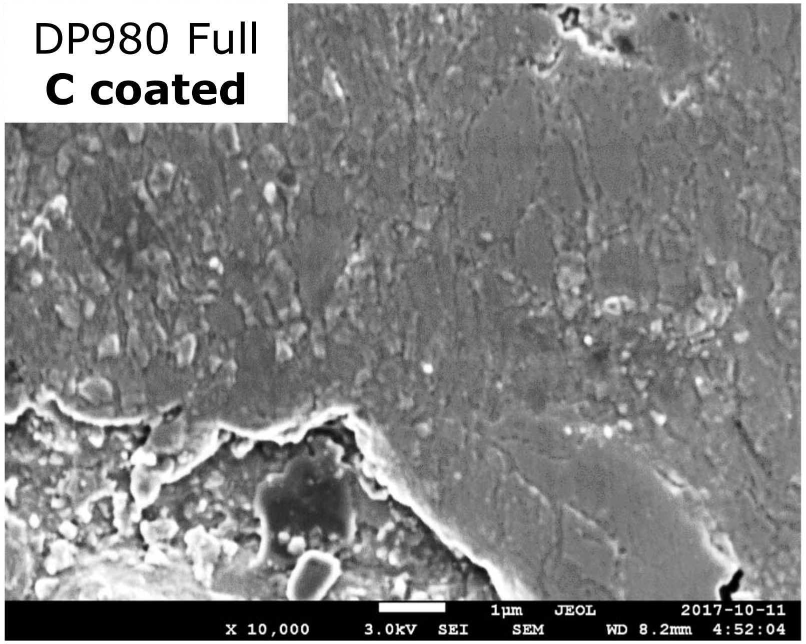

Fig. 15: SEM image of DP980 Full DP-30°C, carbon coated.

- Spatial resolution may not be optimized on our micrographs due to the poor conductivity of surface oxide.
- Coating the samples with a 10nm carbon layer does not improve resolution.
  → Coating with Pt or Au will be tried.

2.2 Oxide morphology

DP780 "A"

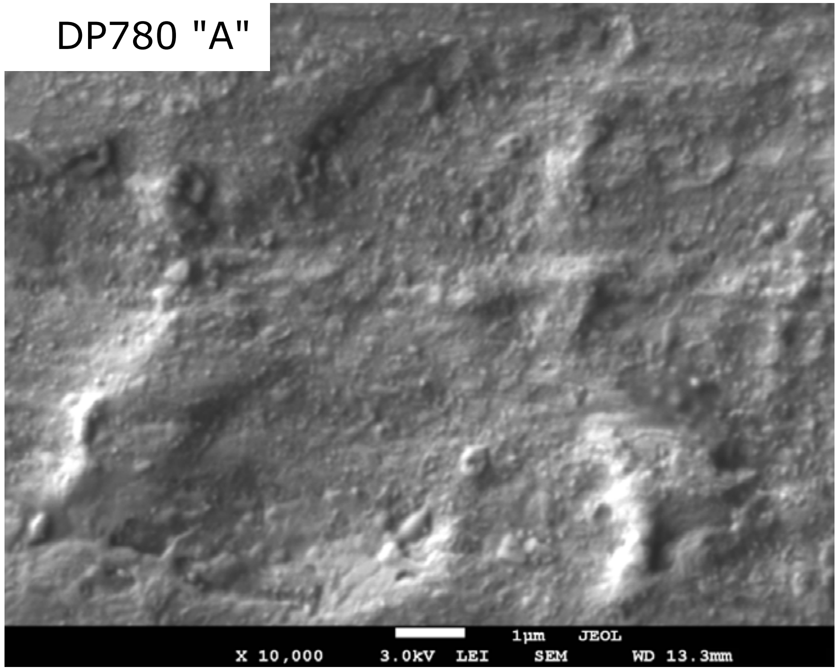

Fig. 16: SEM image of DP780 "A" with LEI detector.

Improving image quality, work performed in collaboration with McMaster

DP780 "Full"

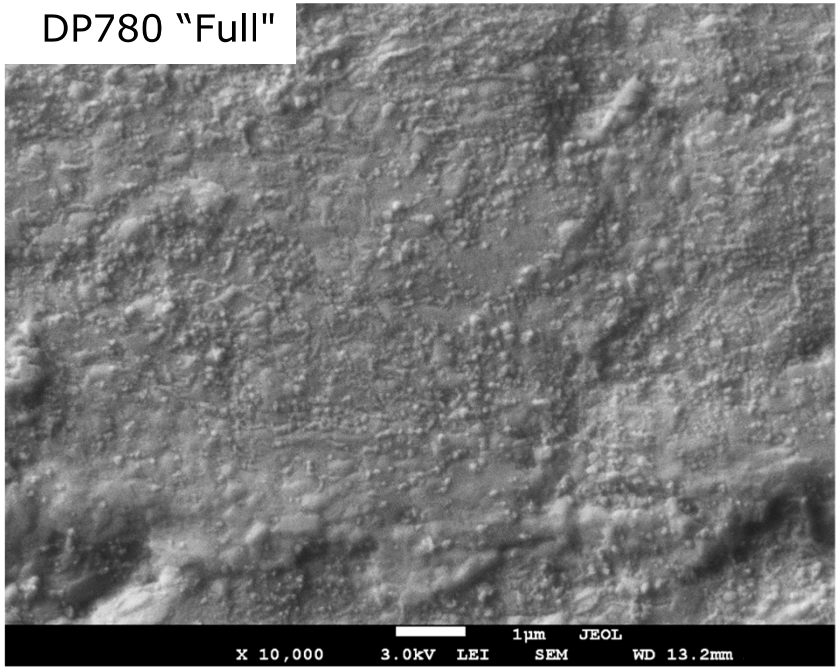

Fig. 17: SEM image of DP780 "Full" with LEI detector.

- Better resolution in lower secondary electron image mode (LEI).
- Secondary electrons only mode → topography contrast.
- The number of oxide islands increases with heating time

2.3 Roughness

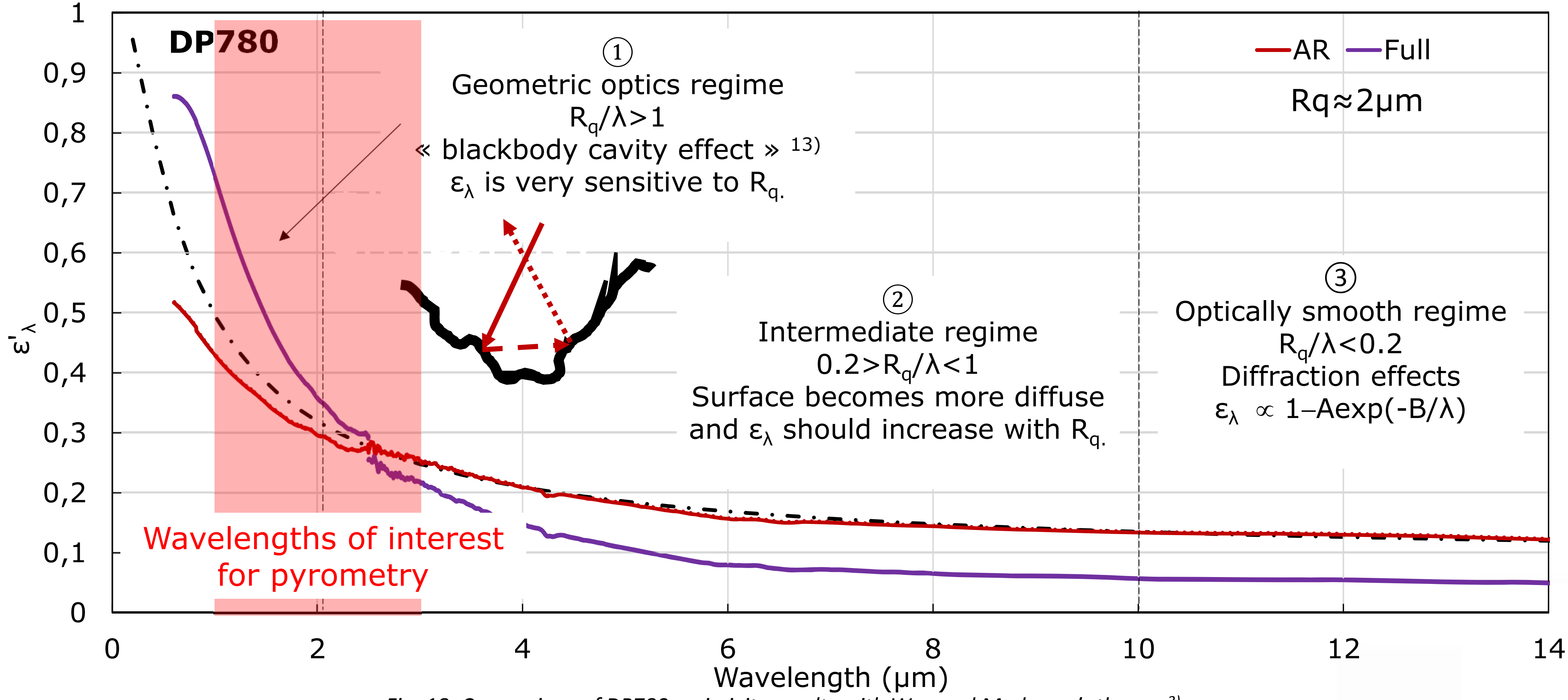

Fig. 18: Comparison of DP780 emissivity results with Wen and Mudawar's theory. [3]

3) C.-D. Wen and I. Mudawar, "Modeling the effects of surface roughness on the emissivity of aluminium alloys," *International Journal of Heat and Mass Transfer*, no. 49, pp. 4279-4289, 2006.

2.3 Roughness

Different techniques were tried to measure roughness evolution:

- Contact pofilometry: Suftest SJ-210
- White light interferometry: Fogale nanotech Photomap 3D and Bruker Contour GT
- Atomic forc

DP780CR AR

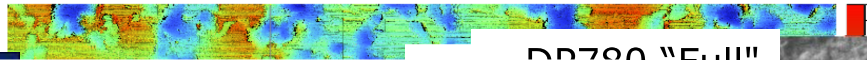

DP780 "Full"

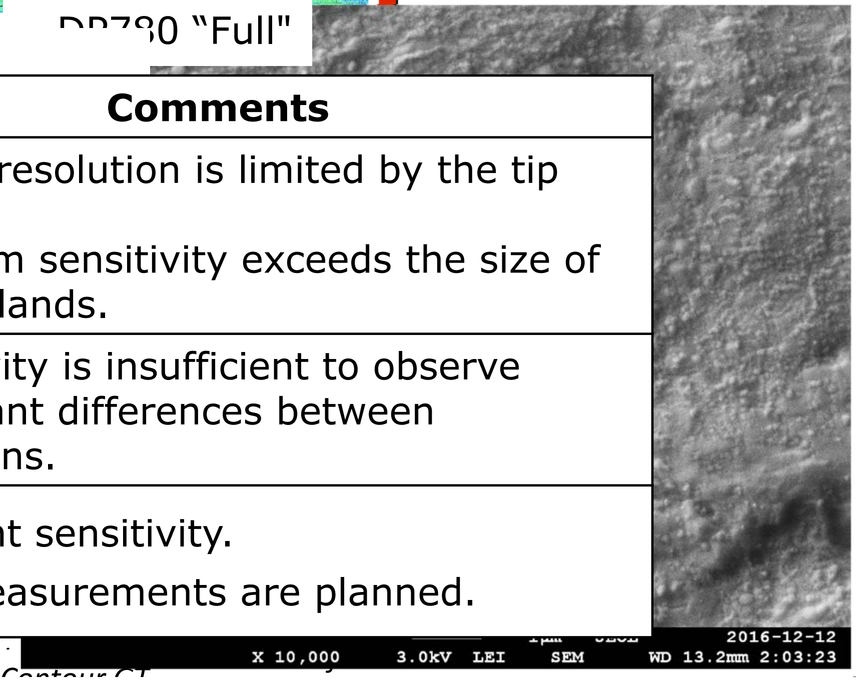

DP78

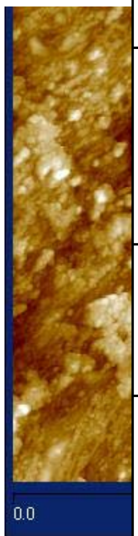

Table 6: Comparison of the different roughness measurement methods.

Technique	Sensitivity	Comments
Contact profilometry	4 µm	• Spatial resolution is limited by the tip radius. • Minimum sensitivity exceeds the size of oxide islands.
White light interferometry	200 nm	• Sensitivity is insufficient to observe significant differences between conditions.
Atomic force microscopy	nm to Å	• Excellent sensitivity. • New measurements are planned.

Fig. 19: Presentation of th

Fig. 22: Surface imaging with AFM for DP780.

Fig. 17: SEM image of DP780 "Full" with LEI detector.

2.3 Roughness

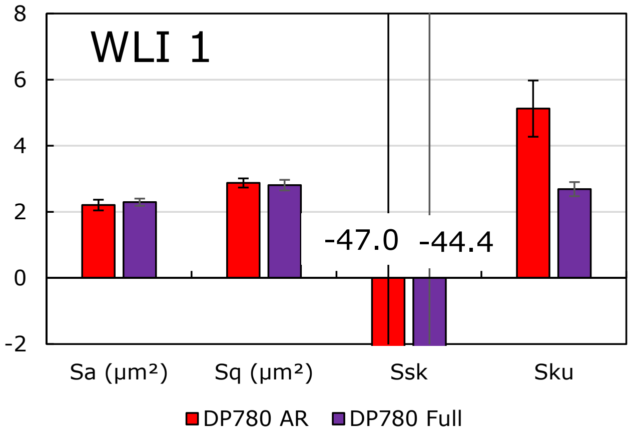

Fig. 21: Results of the first WLI (630x470µm).

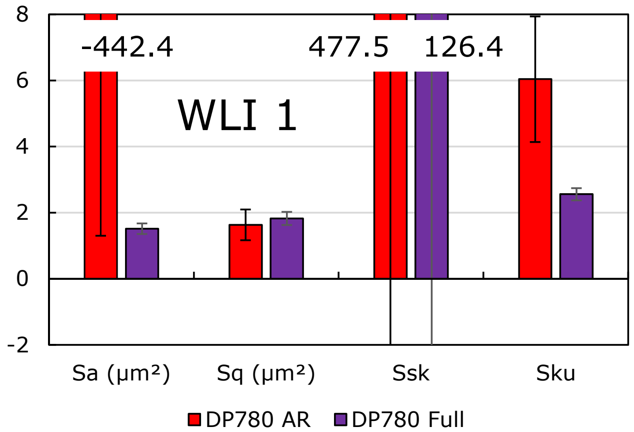

Fig. 22: Results of the first WLI (200x150µm).

WLI 1: Photomap 3D by Fogale nanotech

- Inconsistent results
- Measurement aberrations
- Low spatial resolution (820 and 250nm)

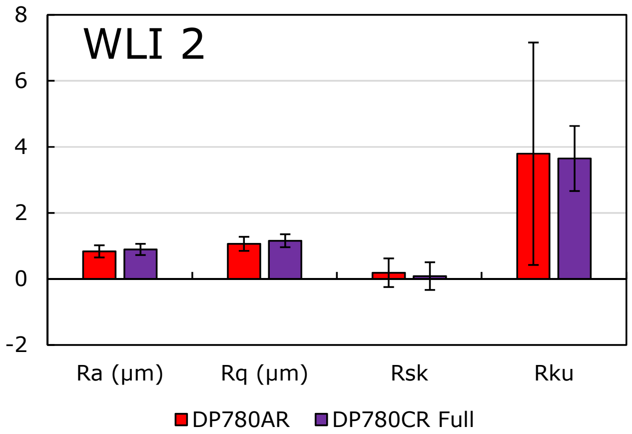

Fig. 23: Results of the new WLI (1x1.2mm).

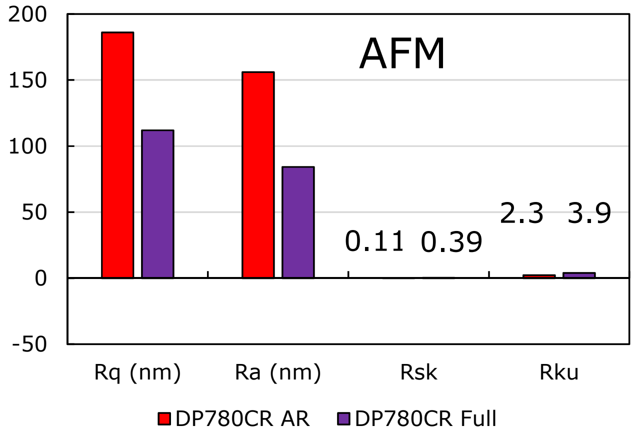

Fig. 24: Results of the AFM (40x40µm).

WLI 2: Contour GT by Bruker

- Large scanning zone with better resolution (200nm)
- No variation trend is observed

AFM

- Only one measurement was performed so far
- Odd results, requires more investigation

2.3 Roughness

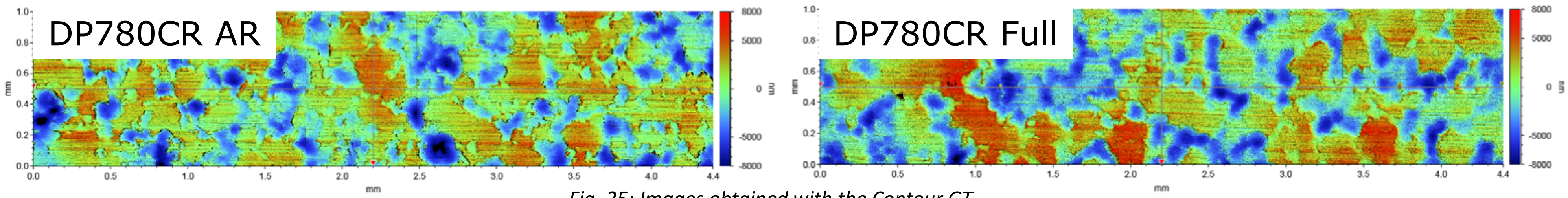

Fig. 25: Images obtained with the Contour GT.

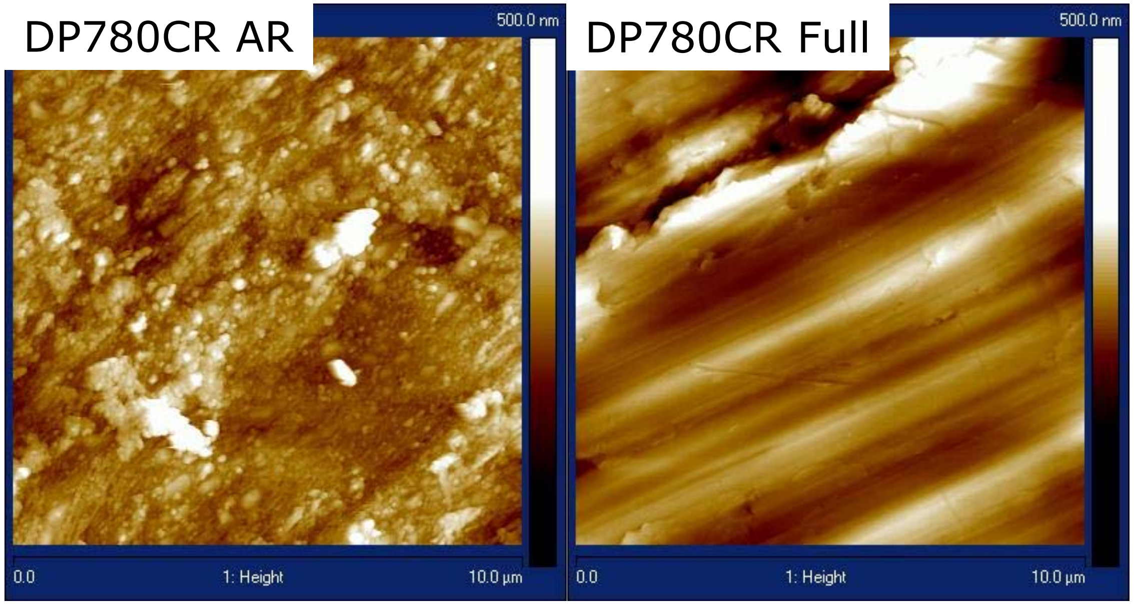

Fig. 26: Images obtained with the AFM.

- No significant difference was observed using the WLI Contour GT.
- AFM showed odd results: samples of "Full" are expected to be rougher than as received material.

  → New measurements are in progress.

2.4 Chemical profiles

We are expecting new GDOES results for:

- DP780CR AR
- DP780CR B
- DP780CR Full DP 0°C
- DP980CR AR
- DP980CR Full DP 0°C

3.1 Galvanized steel observation

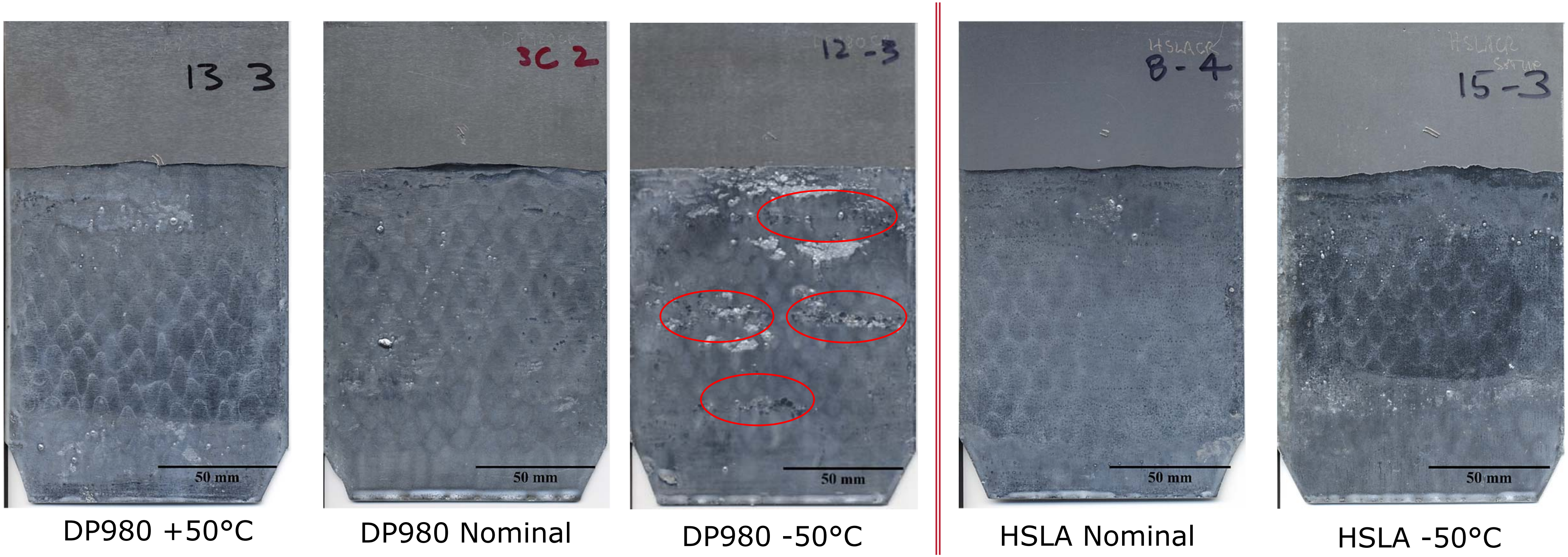

Fig. 23: Galvanized steel sheet surface observations of DP980 and HSLA.

- For all conditions the coating is rough, and has gritty appearance and swollen areas.
- Defects are visible on galvanized steel.
- For -50°C condition, there is more partial coating (circled in red) then for other conditions. This can be due to another type of oxide forming on the surface during heat treatment.

3.2 Tensile test DP980

DP980CR

Table 7: Tensile properties (partial results) of DP980 and HSLA.

Steel	HT	$R_{e0,2}$ [MPa]	R_m [MPa]	A [%]
DP980	+50°C	800	1140	12,0
	Nominal	705	1096	12,4
	-25°C	538	1023	17,0
	-50°C	488	984	15,0
HSLA	Nominal	365	693	28,0
	-50°C	338	668	26,0

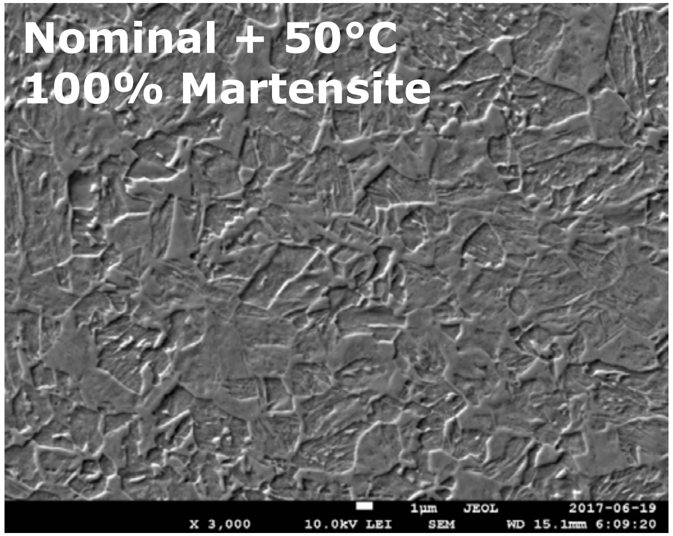

Fig. 24: SEM observation of DP980 at +50°C condition (bare specimen).

- Partial results, analysis in progress.
- The acceptable temperature deviation is below 25°C. This is different from the results presented for bare specimens.

3.2 Tensile test DP980

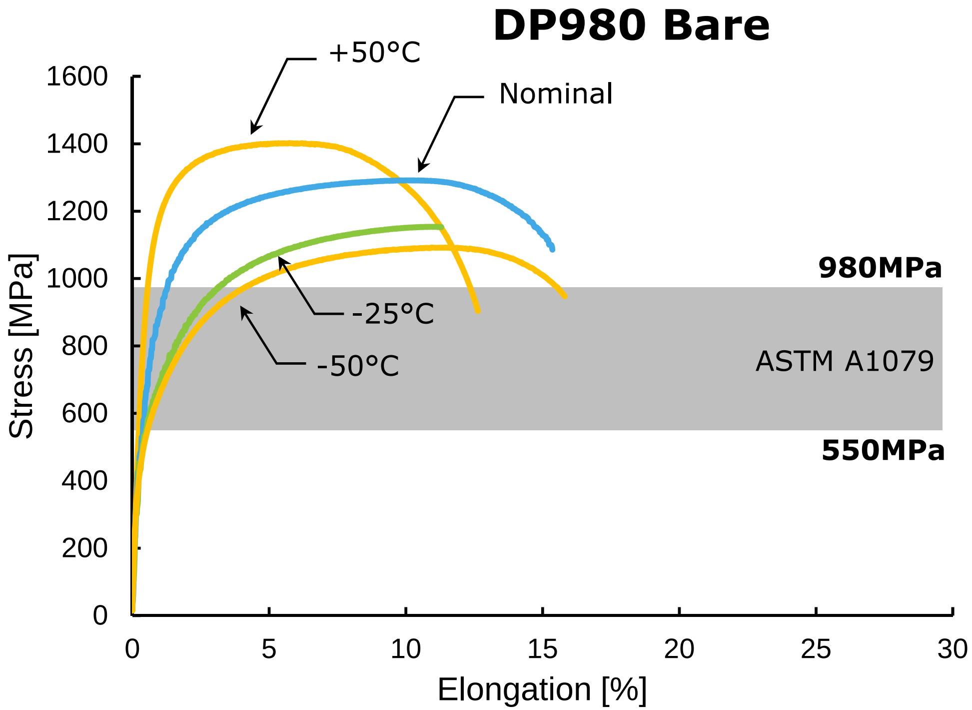

Fig. 25: Typical stress-strain curves for DP980 bare.

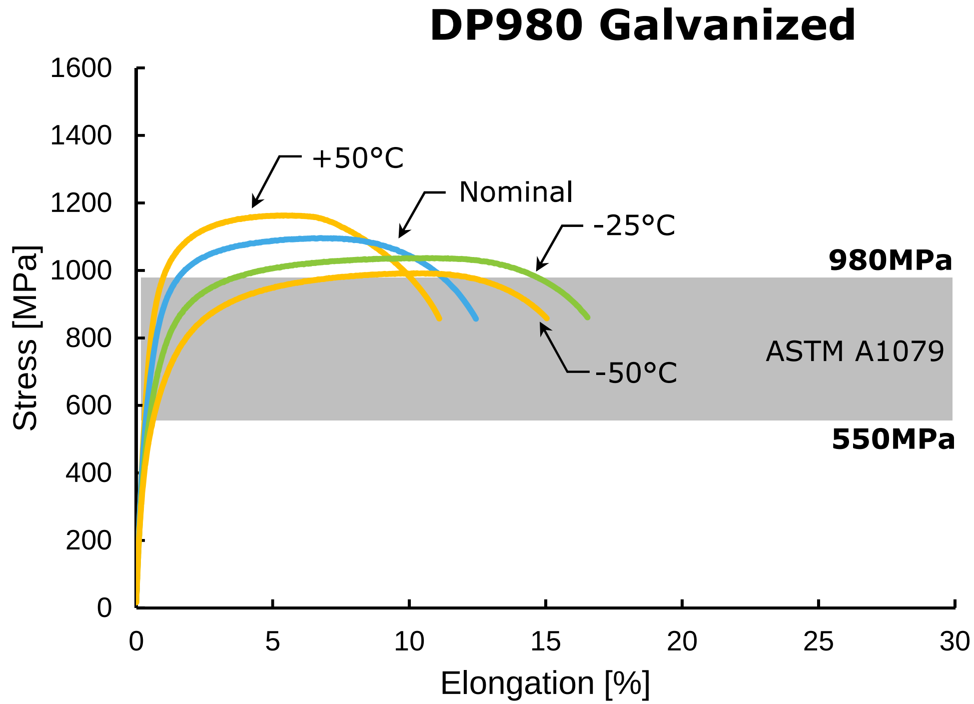

Fig. 26: Typical stress-strain curves for DP980 galvanized.

- There is significant difference in mechanical properties between galvanized and bare steels.
- Microstructural examination is needed.

3.2 Tensile test HSLA

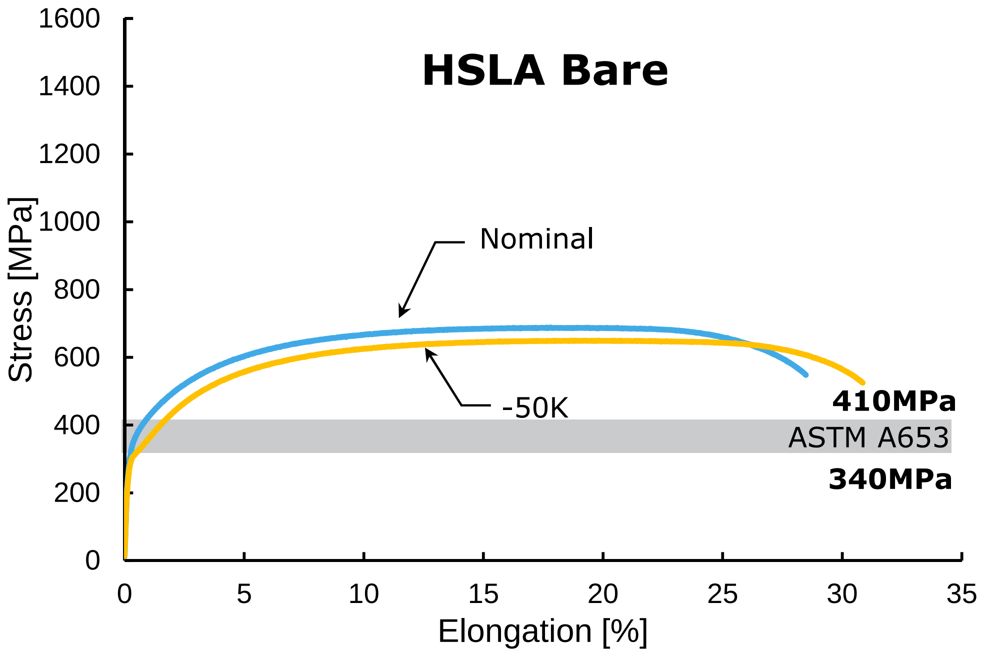

Fig. 27: Stress-strain curves for HSLA bare.

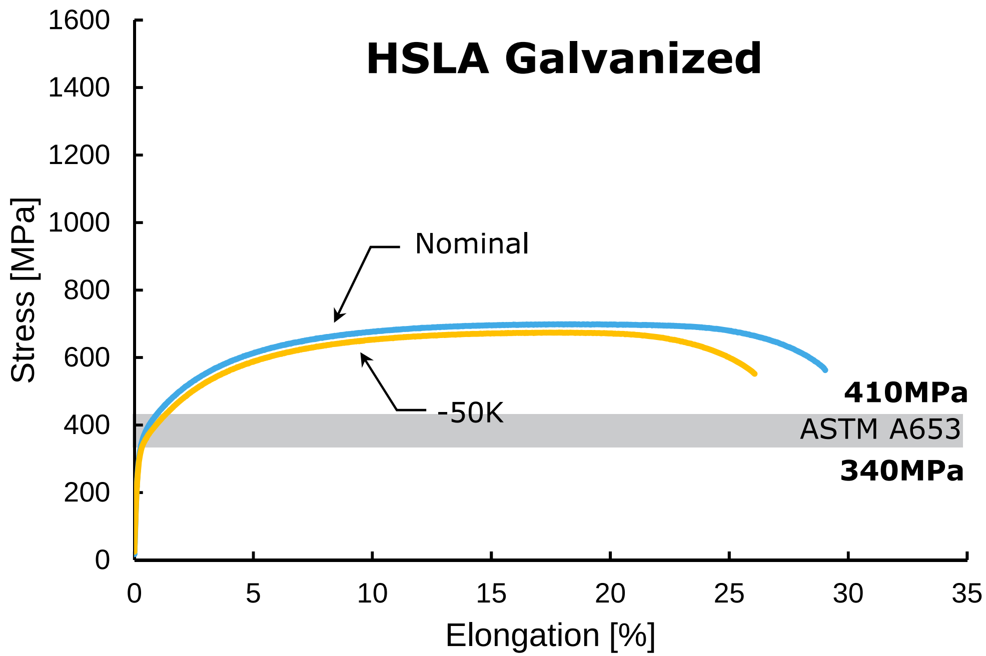

Fig. 28: Stress-strain curves for HSLA galvanized.

- There is no significant difference in mechanical properties between galvanized and non galvanized steels.
- The mechanical properties of HSLA are less sensitive to temperature differences.

3.3 Bend test DP980 and HSLA

Fig. 29: Bend test at 90° for DP980.

Table 8: Sheet thickness and radii for cold bending for DP980 and HSLA.

Steel	Sheet Thickness [mm]	Radius [mm]
HSLA CR	1.8	5.4
DP980 CR	1.5	4.5

Table 9: Bend test results for DP980 and HSLA.

Heat Cycle	-50°C	-25°C	Nominal	+50°C
DP980				
HSLA		N/A		N/A

Table 10: Images of DP980 bent specimens

Nominal heat cycle	+50°C deviation
 No steel cracking No zinc flaking	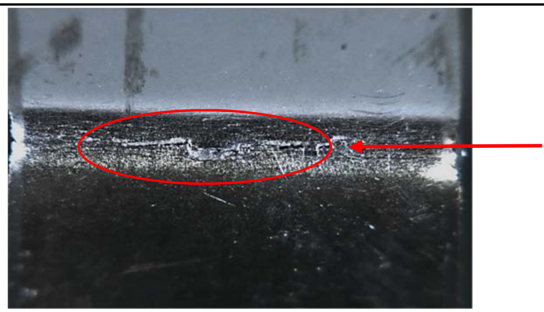 Steel cracks Zinc adheres to the surface

+50°C heat cycle: despite the elongation meets ASTM requirement, the formability is critical.

3.4 Coating evaluation preliminary

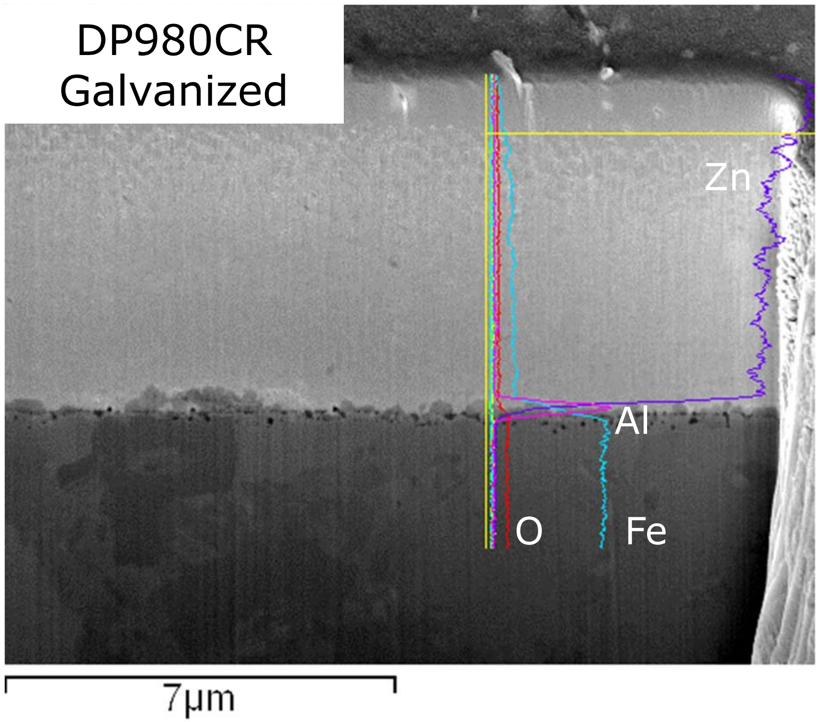

Fig. 30: EDS profile after a test cut with FIB on DP980CR galvanized.

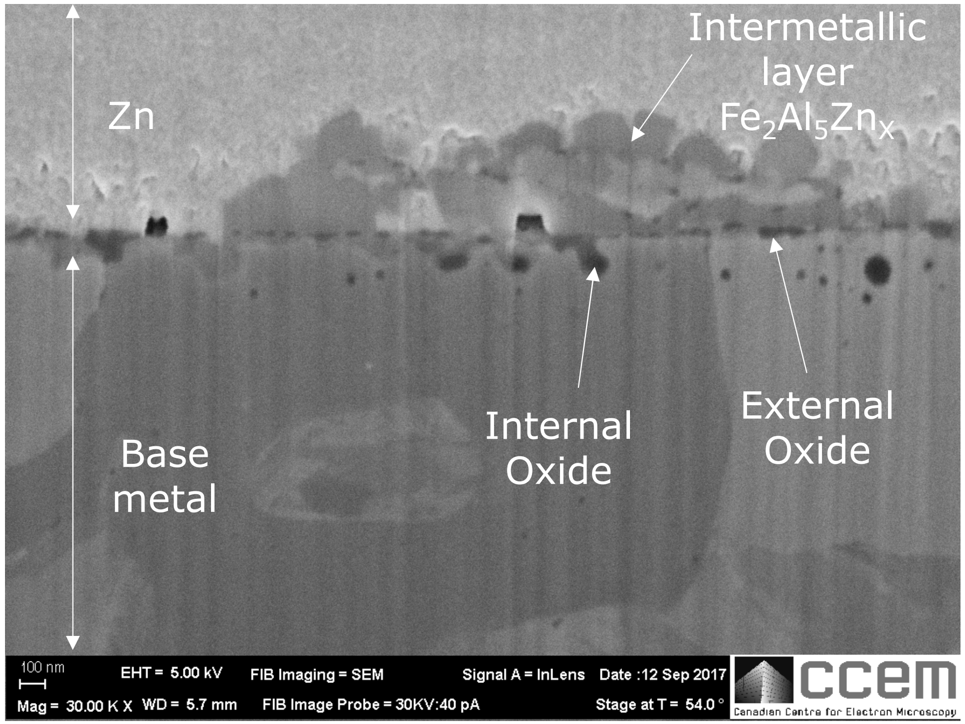

Fig. 31: Observation of the oxide layer of DP980CR galvanized.

- Cross sectional polisher was tried without success.
- FIB gave excellent results to obtain a cross section of the coated specimen.
- Zn layer was measured and is around 6µm thick.
- It is possible to observe the internal oxide network using SEM within FIB.

4. Progress

	Description of milestones	Completion date
1)	**Design of experiments (DOE)**	100 % April 2015
2)	**Acquisition of as rolled samples (hot rolled and cold rolled**	100 % March 2015
3)	**Preliminary Phase: Characterization of the as rolled samples**	100 % May 2016
4)	**Revision of the DOE according to the measured characteristics**	100 % October 2016
5)	**PHASE I : Variation in emissivity and ΔT errors** • Roughness characterization – 90% additionnal measurements by AFM needed • Oxide characterization – 95% • Emissivity measurements - 100 %	Quentin's Thesis December 2017
6)	**PHASE II : Allowable ΔT deviations based on mechanical properties** • In depth microstructural evaluation – 100 % • All other experimental tasks - 100 %	Paul's Thesis December 2017
7)	**PHASE III: Effect of temperature deviation on Zn adhesion** • Sample production – 100 % (received in March 2017) • Tensile and bend tests – 80 % • Examination of oxide/coating microstructure – 1%	December 2017
8)	**Modelling – 15%**	ZCO-72 (2017-2020)
9)	**Redaction of final report and results dissemination + GAP meeting**	Winter 2018

5. ZCO-72 project (2017-2020)

Enhanced Pyrometry for Continuous Galvanizing of Advanced High Strength Steel

PI: Kyle Daun, University of Waterloo, Co-applicants: Myriam Brochu (Polytechnique)
HQP: Simon Trivett (M1), Kaihsiang Lin (D1), Marina Pushkareva (PD1), TBD (M2)

TASK I : Elucidate the relationship between the surface state/AHSS composition and spectral emissivity (Trivett, Lin, Waterloo)

TASK II: Link the uncertainty in spectral emissivity to mechanical properties and zinc layer adhesion of AHSS strip (Pushkareva, Student M2, Polytechnique)

TASK III: Incorporate knowledge gained from Task I and Task II into a pyrometry algorithm (Lin, Waterloo)

international zinc association | STELCO The Steel Company of Canada | Williamson Where Wavelength Matters | SRB Controls Inc Industrial Instrumentation Specialists | NSERC CRSNG | Ontario Centres of Excellence Where Next Happens

Task I: Relationship between surface state and ε_λ

- Phase I highlighted relationship between ε_λ and surface roughness/oxide through ex-situ measurements

Activities:

- Construct chamber for in-situ ε_λ measurements from AHSS undergoing heating
- Precise control of surface temperature, atmosphere (DP)
- Ex-situ surface characterization through GDOES, XRD, SEM
- Roughness measurements through optical profilometry, AFM

Key objectives/questions:

- How do CGL process parameters affect ε_λ? Can we develop a phenomenological model?
- How do defects (e.g. pickling stains, scratches) affect ε_λ?

Simon Trivett

Kaihsiang Lin

Task I: Construction of measurement chamber

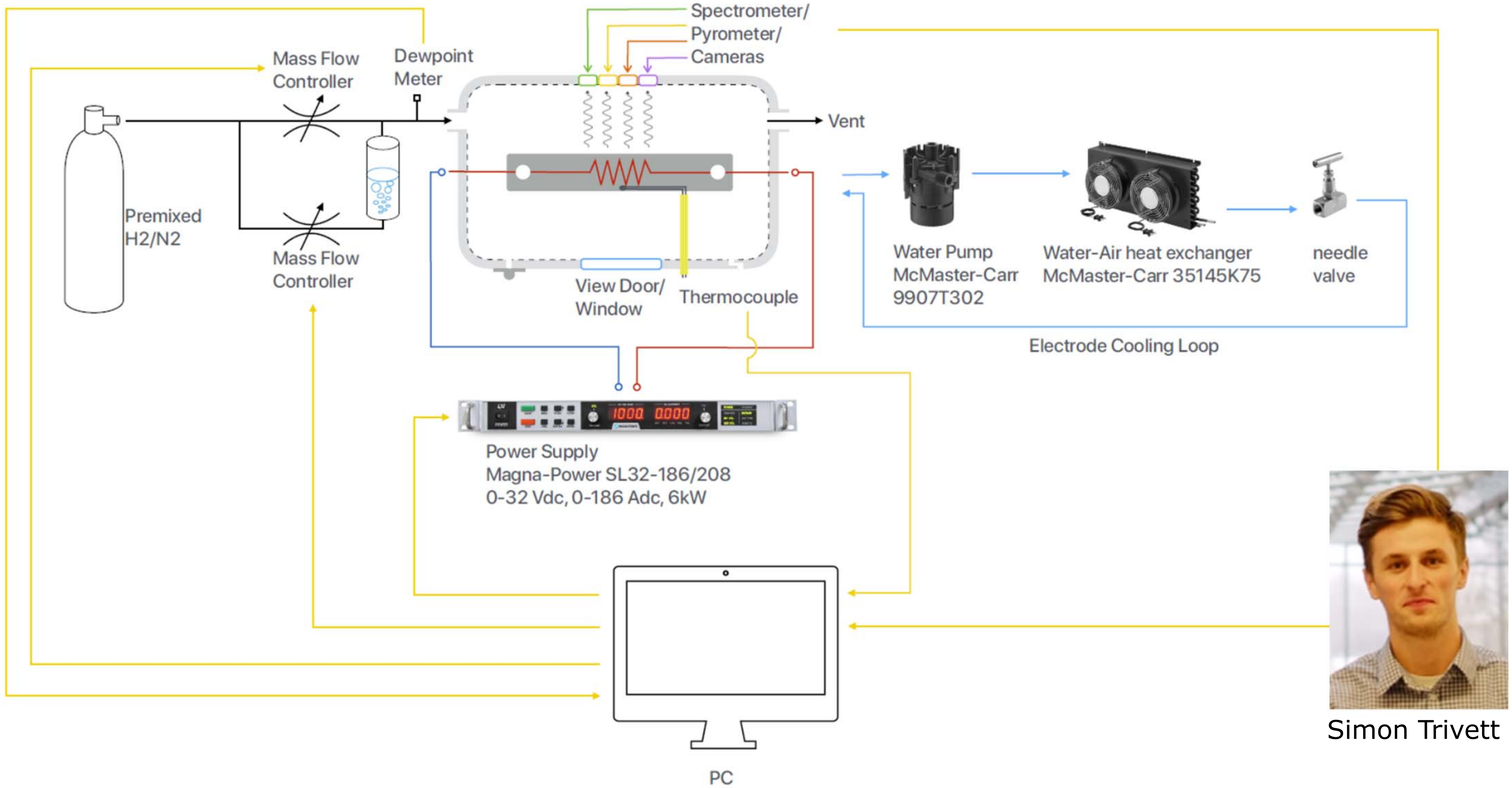

Simon Trivett

Task II: Link between ΔT and AHSS properties

- Phase II confirmed that pyrometry errors caused by uncertain ε_λ is at least partially responsible for high AHSS rejection rates

Activities:

- Extend analysis to consider more alloy compositions, annealing temperatures, heating and cooling rates
- Gleeble dilatometry measurements
- Comparison with CALPHAD-type models (e.g. JMatPro) derived from phase equilibrium data

Key objectives/questions:

- Relate annealing schedule excursions to variations in mechanical properties and microstructure
- Derive an annealing schedule envelope that ensures AHSS properties are within specification

Marina Pushkareva

Task III: Improved pyrometry for CGLs

- Transfer of knowledge from Tasks I and II to industry

Activities:

- Work closely with Stelco and Williamson/SRB to improve existing pyrometry methods on CGLs
- White box, black box, and grey box models derived from ε_λ measurements made through Task I
- Determine optimal detection wavelengths through DOE theory

Key objectives/questions:

- Derive robust uncertainties using Bayesian methodology
- Data synthesis to reduce uncertainties below intervals found through Task II
- Use pyrometry measurements for fault/defect detection

Kaihsiang Lin

Proposed timeline

	2017			2018			2019			2020		
Task 1: Relationship between ε_λ and surface phase (Waterloo)												
Chamber design and construction (ST)												
Sample processing (ST, KL, MP)												
Ex situ analysis (KL, ST, MP)												
Task 2: Relationship between ΔT and AHSS material props. (Polytechnique)												
Process samples in McMaster simulator (MP, M1)												
Gleeble measurements (MP, M1, KL)												
Surface phase sensitivity to Mn/Si (MP, M1)												
CALPHAD model development (MP)												
Task 3: Pyrometry algorithms/industrial implementation (Waterloo)												
Review of existing pyrometry techniques (KL)												
Development of white/black/grey box models (KL)												
Defect detection (KL)												
Industrial implementation (KL)												

Planned budget

	2018	2019	2020	Total
IZA-GAP (cash)	$66,000[1]	$66,000	$66,000	**$198,000**
University overhead	$11,920	$11,920	$11,920	**$35,759**
Total in-kind	$40,000	$34,000	$34,000	**$108,000**
NSERC (cash)	$94,080	$88,080	$88,080	**$270,241**
Total cash	$148,161	$142,161	$142,161	**$432,482**
Total budget (cash+in kind)	**$188,161**	**$176,161**	**$176,161**	**$540,482**

OCE VIP II (proposed)	$75,000[2]	$75,000[2]	$0	**$150,000**
Total cash	**$233,161**	**$217,161**	**$142,161**	**$592,483**
Total budget (cash+in kind)	**$263,161**	**$251,161**	**$176,161**	**$690,483**

Notes:
1. $55,000 USD≈$66,000 CDN
2. OCE VIP II maximum match of $37,500 K cash + $37,500 K in kind over two years
3. Total leveraging with NSERC = 2.2:1, total leveraging with NSERC/OCE = 3:1

POLYTECHNIQUE
MONTRÉAL

UT TENSIO SIC VIS

WORLD-CLASS
ENGINEERING

THANK YOU !

References

1. E.M. Bellhouse, A.I.M. Mertens, J.R. McDermid, “Development of the surface structure of TRIP steels prior to hot-dip galvanizing”, Mat. Sc. and Eng. A, 463, 2007

2. I-R. Sohn, J-S. Kim, S. Sridhar “Effect of Dew points and Gas Flow Rate on the Surface Oxidation of Advanced High Strength Steels“, ISIJ Int., Vol. 55(2015), No. 9.

3. C.-D. Wen and I. Mudawar, "Modeling the effects of surface roughness on the emissivity of aluminium alloys," *International Journal of Heat and Mass Transfer*, no. 49, pp. 4279-4289, 2006

Comparison heat cycle Phase 2 and Phase 3

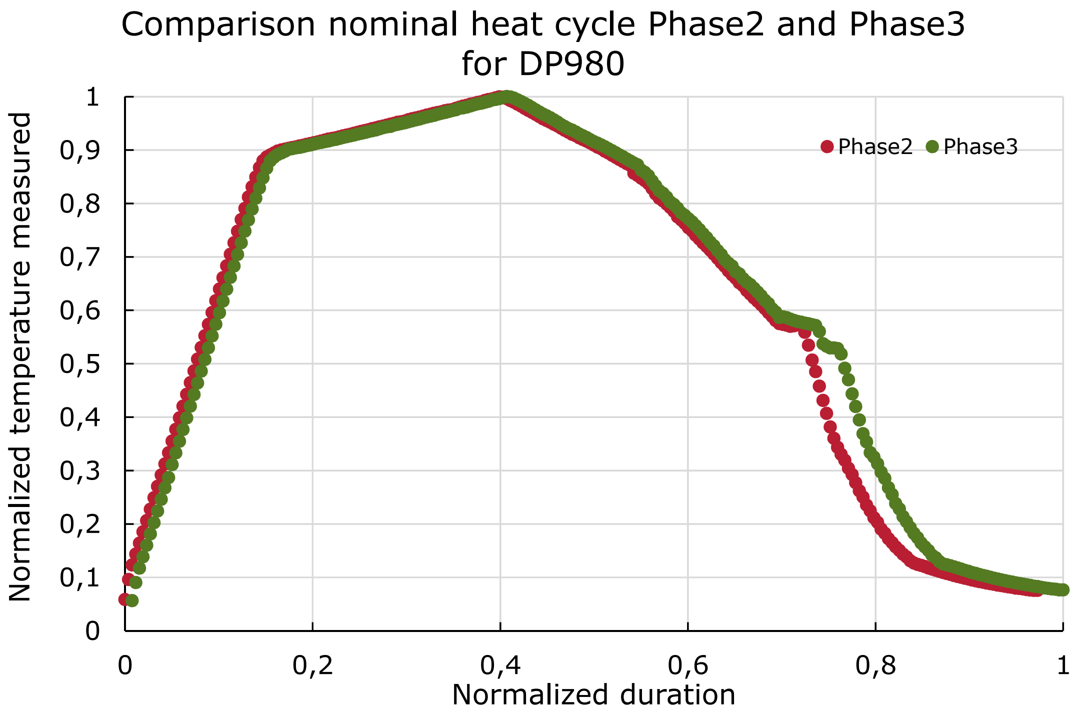

Thermocouple data

Heat cycle difference is due to zinc immersion during phase3.
6s delay between phase 2 and 3 for a temperature below 460°C.
According to JMatPro, Ms < 400°C ➔ Austenite decomposition continue during zinc immersion